Rivista Italiana di Paleontologia e Stratigrafia	volume 109	no. 2	3 pls.	pp. 359-376	June 2003

CYCLIC SEDIMENTATION ACROSS THE PERMIAN - TRIASSIC BOUNDARY (CENTRAL TAURIDES, TURKEY)

EMRE ÜNAL*, DEMIR ALTINER*, İ. ÖMER YILMAZ* & SEVINÇ ÖZKAN-ALTINER*

Received March 15, 2002; accepted February 5, 2003

Key Words: Meter-scale cyclicity, Permian-Triassic boundary, foraminifera, microfacies, hiatus, highstand systems tract, transgressive systems tract.

Abstract. The best preserved Permian - Triassic boundary beds in Turkey are found in the Hadim region of the central Taurides. The succession is exposed in one of the allochthonous units of the Tauride Belt, the Aladağ Unit, whose stratigraphy includes beds ranging from the Devonian to the Cretaceous systems. In the Aladağ Unit, the Permian-Triassic boundary beds are entirely composed of carbonates. The Permian portion of these beds belongs to the *Paradagmarita* Zone, whereas the lowermost Triassic contains the Lower Griesbachian marker *Rectocornuspira kalhori*. The uppermost Permian carbonates, composed of meter-scale upward shallowing subtidal cycles, are characterized by oolitic limestones of regressive character at the top and are overlain sharply by Lower Triassic stromatolites. Cyclic Upper Permian carbonates are interpreted as highstand sytems tract deposits of the last third-order sequence of the Permian System. The Permian-Triassic boundary is an unconformity corresponding to both erosional and non-depositional hiatuses. The gap at the Permian-Triassic boundary partially corresponds to the shelf-margin systems tract and partly to the transgressive systems tract of the overlying third-order sequence. Stromatolites are interpreted as transgressive systems tract deposits.

Riassunto. La successione intorno al limite Permiano-Triassico della regione di Hadim nei Tauri Centrali sembra essere la migliore sinora descritta in Turchia. La successione affiora in una delle unità alloctone della catena dei Tauri, l'unità Aladağ, in cui sono presenti formazioni che vanno dal Devoniano al Cretaceo. Nell'Unità Aladağ, gli strati Permo-Triassici sono composti interamente da carbonati. La parte permiana della successione appartiene alla zona a *Paradagmarita*, mentre il Triassico basale contiene la specie-indice del Griesbachiano inferiore *Rectocornuspira kalhori*. Le rocce carbonatiche del Permiano sommitale sono formate da cicli metrici subtidali con tendenza verso l'emersione e sono caratterizzate da calcari oolitici a carattere regressivo alla sommità, per venire ricoperte con contatto netto da stromatoliti del Triassico inferiore. I carbonati ciclici del Permiano superiore sono interpretati come depositi di stazionamento alto dell'ultima sequenza di terzo ordine del Sistema Permiano. Il limite Permiano-Triassico corrisponde ad una discontinuità in corrispondenza di una lacuna sia erosionale che deposizionale. La lacuna al limite Permiano-Triassico corrisponde parzialmente al system tract del margine della piattaforma e in parte al tratto trasgressivo della soprastante nuova sequenza di terzo ordine. Le stromatoliti sono interpretate come depositi del sistema trasgressivo.

Introduction

The central Tauride Belt (Fig. 1) is characterized, in general, by an autochthonous unit (Geyik Daği Unit; Özgül 1976) ranging in age from Cambrian to Eocene and nappes overlying this autochthon (allochthonous units of the Tauride Belt) transported hundreds of km from the north and the south (Blumenthal 1947, 1951; Özgül 1971, 1976, 1984, 1997). The Aladağ Unit, representing one of the allochthonous units and exposed along the NW-SE trending structure of the belt, was thrusted onto the autochthon during Eocene time and displays the most complete Upper Paleozoic marine successions in Turkey (Özgül 1976, 1997; Altiner 1981, 1984, Altiner et al. 2000; Altiner & Özgül 2001). The Upper Paleozoic deposits of the Aladağ Unit are best observed in a locality 20 km south of the town of Hadim (Figs. 1, 2). The Permian succession of the Hadim-Taşkent area was named the Çekiç Daği Formation (Özgül 1997) and divided into four mappable members (Fig. 2). The lower three members (Keltaş, Çamalan and Kizilgeriş), consisting of fusuline-bearing oncolitic and micritic limestones and quartzarenitic sandstones, are Asselian to Middle Permian (Midian) in age according to Altiner & Özgül (2001). The uppermost Yellice Member is a thick carbonate deposit of Midian (=Capitanian according to the Standard Permian Scale; Jin et al. 1997) to Dorashamian (=Changxingian) age. According to Altiner & Özgül (2001), the Yellice Member is divided into three zones,

* Marine Micropaleontology Research Unit, Department of Geological Engineering, Middle East Technical University, 06531 Ankara, Turkey. E-mail: unemre@metu.edu.tr

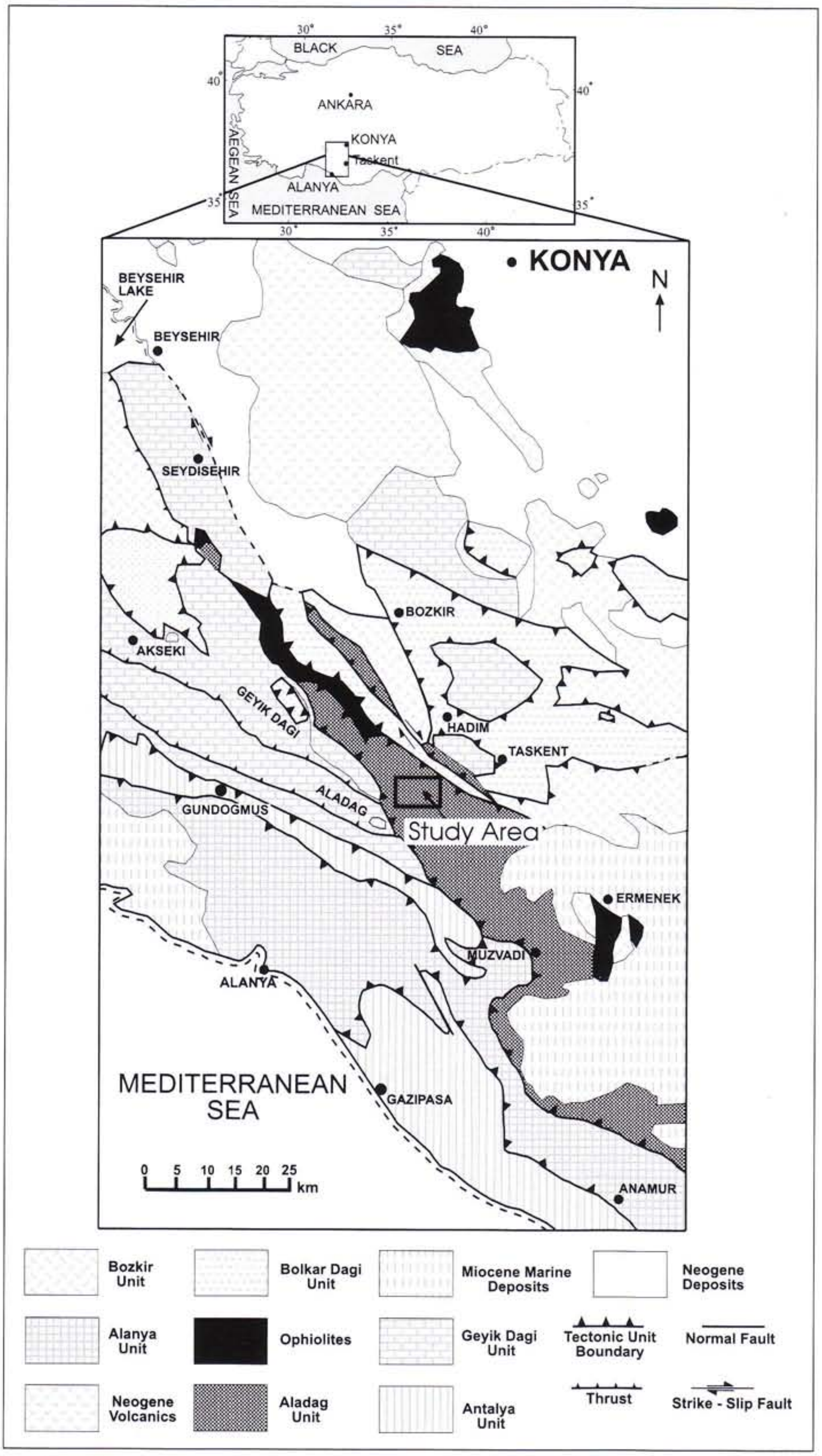

Fig. 1 - Simplified geological map of part of the central Taurides (Özgül, 1984) and the location of the study area.

namely the *Dunbarula* Zone (Midian), *Septoglobivalvulina gracilis* Zone (Djulfian=Wuchiapingian in the Standard Permian Scale; Jin et al. 1997) and the *Paradagmarita* Zone (uppermost Djulfian-Dorashamian).

The Permian-Triassic boundary beds are characterized by three important lithologic changes (Altiner & Özgül 2001) within the Dorashamian Stage. Gray-coloured limestone beds rich in foraminifers and algae are overlain in the last 40 to 60 cm by oolitic limestones with ripple marks. This oolitic level shows evidence of subaerial exposure and is truncated by stromatolites of Early Triassic age.

The extreme base of the stromatolites contains the Lower Griesbachian marker *Rectocornuspira kalhori*, and according to Altiner & Özgül (2001), there is a gap in sedimentation at the boundary.

Evidence for the gap includes the truncation of ripples, the regressive nature of subaerially exposed oolites and the transgressive nature of the stromatolites.

Following the study of Altiner et al. (1980), who described several Permian-Triassic boundary beds including a gap in sedimentation in western Tethys, similar observations were made on the Permian-Triassic boundary beds of the Antalya Nappes by Marcoux & Baud (1986) and Crasquin-Soleau et al. (2002). In the Çürük Dag section, the gap between the regressive oolites and the overlying stromatolites corresponds to the latest Changxingian and the earliest Griesbachian based on ostracod and conodont data (Crasquin-Soleau et al. 2002).

Within the context of this background information, three sections were measured across the Permian-Triassic boundary in order to study the cyclicity and interpret the boundary from a sequence stratigraphical point of view (Figs. 2 and 3; sections 1, 2 and 3).

Each section measures about 10 m in thickness. A total of 160 samples was collected, with samples coming from nearly each bed within the sections.

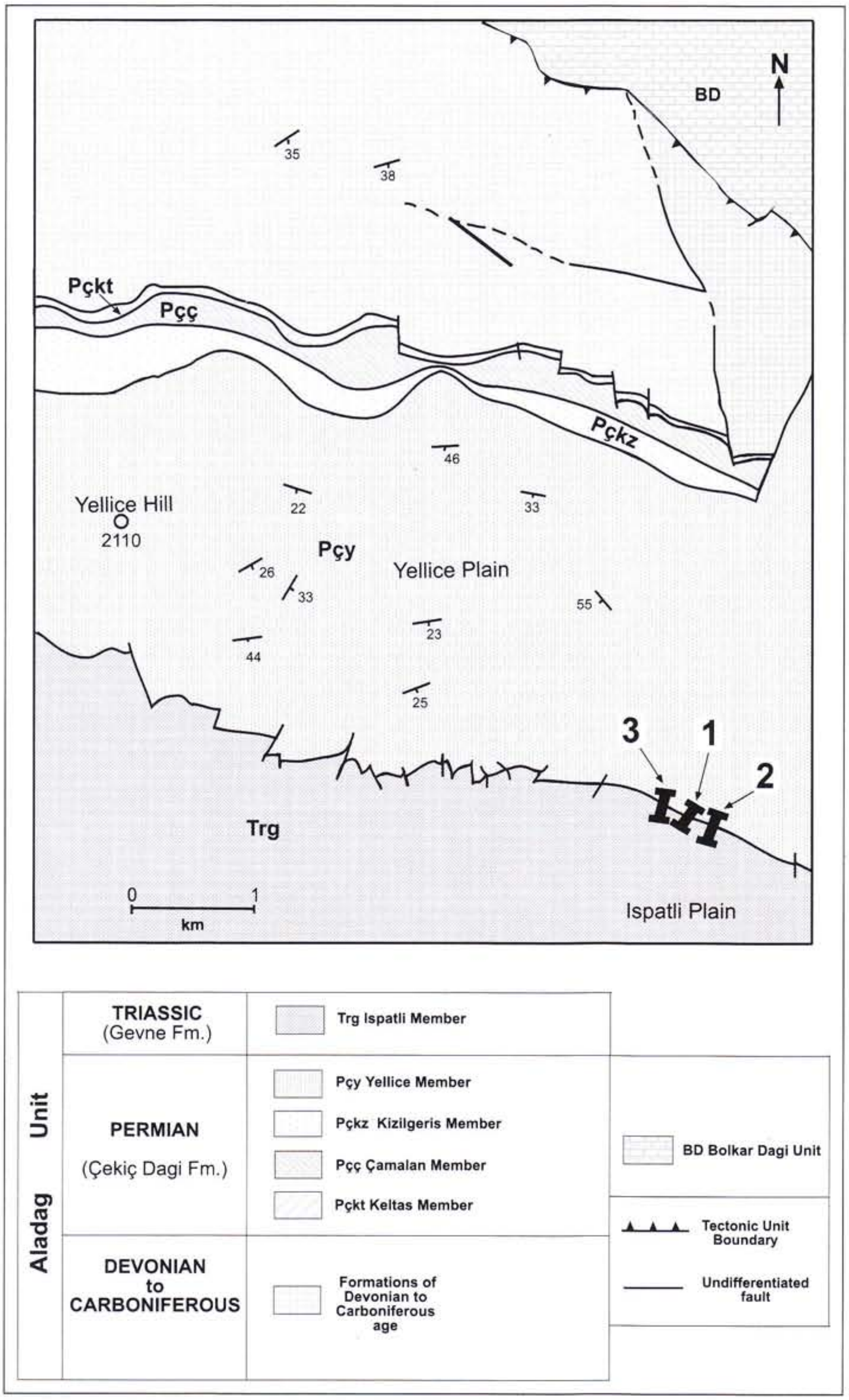

Fig. 2 - Geological map showing Upper Paleozoic and Triassic formations of the Aladağ Unit (20 km south of the town of Hadim) (Altiner & Özgül 2001). 1, 2 and 3 are stratigraphic sections measured across Permian-Triassic boundary beds.

Micropaleontology and microfacies

Three sections measured in this study belong to the uppermost part of the *Paradagmarita* Zone (uppermost Djulfian-Dorashamian) of Altiner & Özgül (2001) and the lowermost part of the Griesbachian stage characterized by *Rectocornuspira kalhori* (Altiner 1981; Altiner & Zaninetti 1981). The micropaleontological analysis of 160 samples collected along these three sections yielded the following foraminiferal fauna from the Permian portion of sections: *Paradagmarita monodi* Lys (Pl. 1, figs. 1-2); *Louisettita elegantissima* Altiner & Brönnimann; *Dagmarita chanakchiensis* Reitlinger (Pl. 1, figs. 3-4); *Globivalvulina decrouezae* Köylüoğlu & Altiner (Pl. 1, figs. 5-8); *G. vonderschmitti* Reichel (Pl. 1, fig. 13); *Globivalvulina-Septoglobivalvulina* transition (Pl. 1, fig. 12); *Septoglobivalvulina gracilis* (Zaninetti & Altiner) (Pl. 1, figs. 9-11); *Pachyphloia* ex gr. *ovata* Lange (Pl. 1, figs. 15-16); *P.* spp. (Pl. 1, figs. 14, 44); *Geinitzina postcarbonica* Spandel (Pl. 1, figs. 17-22); *G. reperta* Bykova (Pl. 1, fig. 31); *Nodosinelloides* spp. (Pl. 1, figs. 23-30); *Frondina permica* Sellier de Civreux & Dessauvagie (Pl. 1, figs. 32-33, 34 ?, 38); *F.* spp. (Pl. 1, figs. 35-36, 39-40); *Ichthyofrondina latilimbata* (Sellier de Civreux & Dessauvagie) (Pl. 1, fig. 37); *Frondinodosaria pyrula* Sellier de Civrieux & Dessauvagie (Pl. 1, fig. 43); *Calvezina* sp. (Pl. 1, fig. 41); *Langella perforata* (Lange) (Pl. 1, fig. 42); *Robuloides lens* Reichel (Pl. 1, fig. 45); *Hemigordius* ? sp. (Pl. 1, fig. 46); *H. zaninettiae* Altiner (Pl. 1, fig. 47); *H.* sp. (Pl. 1, fig. 48); *Multidiscus padangensis* (Lange) (Pl. 1, fig. 49); *Agathammina pusilla* (Geinitz) (Pl. 2, figs. 1-3); staffellids (Pl. 2, figs. 4-8) and *Reichelina* sp. (Pl. 2, fig. 9). In the Lower Triassic portion of the sections, foraminifers are not diversified and comprise only tubular forms represented by *Rectocornuspira kalhori* Brönnimann, Zaninetti & Bozorgnia (Pl. 2, figs. 10-12); *Earlandia* sp. (Pl. 2, fig. 13) and some other unknown foraminifera poorly preserved and very scarce in the stromatolitic facies.

Upper Permian to lowermost Triassic carbonates are characterized by 6 different lithofacies in the measured sections (Figs. 4-5):

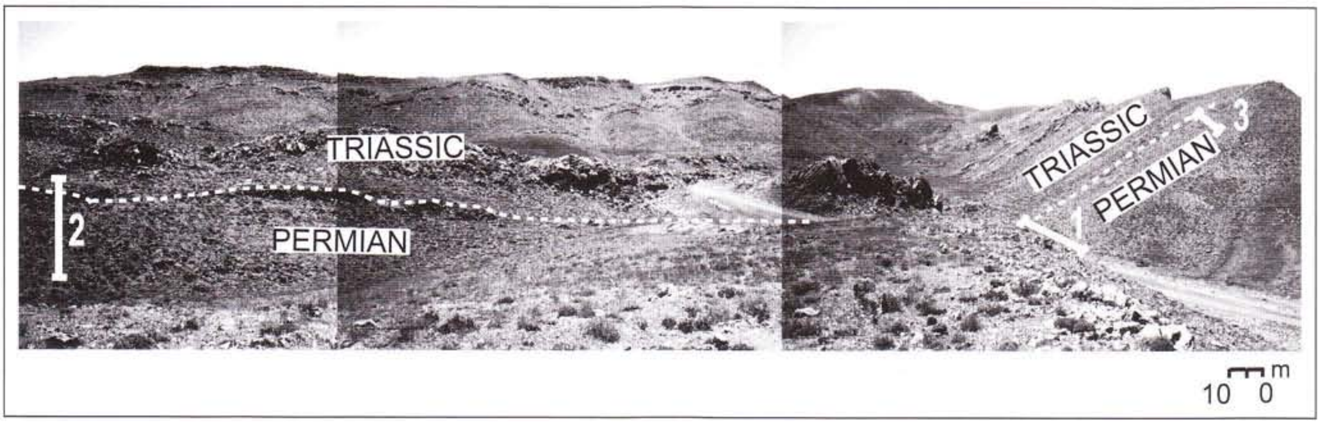

Fig. 3 - Permian-Triassic boundary beds and measured sections (1, 2 and 3).

Algal wackestone-packstone lithofacies: this lithofacies consists of both small broken fragments and large unbroken thalli of algae (mostly gymnocodiacean) embedded in a slightly winnowed micritic groundmass (Pl. 2, fig. 14). The central stem of most gymnocodiacean algae is filled with dark inhomogeneous micrite, usually different than the groundmass, suggesting that algae are mostly allochthonous. Angular-subangular recrystallized grains are abundant in the lithofacies. Most of these are broken pieces of algae, however recrystallized rounded ones resemble algal spores of Flügel (1982) or microspheres of Kershaw et al. (1999).

This lithofacies is composed in places of biosparites (packstones) in which the micritic matrix almost completely washed out (Pl. 2, fig. 19). Large gymnocodiaceans (*Permocalculus*) algae are partly miciritized (coated) and the presence of drusy calcite cement indicates a freshwater diagenetic influence.

Mudstone-packstone lithofacies with oncolites and dark clasts: this lithofacies partly resembles the algal wackestone-packstone lithofacies (Pl. 2, fig. 15). The chief difference, however, is the presence of dark, alloch-

PLATE 1

Fig. 1-2 - *Paradagmarita monodi* Lys. Section 1, 1: sample 4; 2: sample 21. 1-2: X95.

Fig. 3-4 - *Dagmarita chanakchiensis* Reitlinger. Section 1, 3: sample 2; 4: sample 3. 3: X95; 4: X140.

Fig. 5-8 - *Globivalvulina decrouezae* Köylüoglu & Altiner. Section 3, 5: sample 64; 7: sample 79. Section 1, 6: sample 33. Section 2, 8:sample 63. 5, 7: X95; 6: X70; 8: X115.

Fig. 9-11 - *Septoglobivalvulina gracilis* (Zaninetti & Altiner). Section 3, 9: sample 135. Section 1, 10: sample 41; 11: sample 18. 9-11: X70.

Fig. 12 - *Globivalvulina-Septoglobivalvulina* transition. Section 1, sample 17, X35.

Fig. 13 - *Globivalvulina vonderschmitti* Reichel. Section 1, sample 5, X70.

Fig. 14, 44 - *Pachyphloia* spp. Section 2, 14: sample 74. Section 3, 44: sample 121. 14: X80; 44: X95.

Fig. 15-16 - *Pachyphloia* ex gr. *ovata* Lange. Section 1, 15: sample 38. Section 2, 16: sample 79. 15-16: X95.

Fig. 17-22 - *Geinitzina postcarbonica* Spandel. Section 3, 17: sample 131; 18: sample 124; 19: sample 121; 20: sample 102. Section 1, 21: sample 35; 22: sample 34. 17-18: X95; 19-20: X110; 21: X105; 22: X160.

Fig. 23-30 - *Nodosinelloides* spp. Section 2, 23: sample 5; 24: sample 56. Section 3, 25-26: sample 121; 27: sample 109; 28: sample 116; 29-30: sample 124. 23: X120; 24, 28-30: X95; 25: X200; 26-27: X85.

Fig. 31 - *Geinitzina reperta* Bykova. Section 2, sample 74, X95.

Fig. 32-33, 34 ?, 38 - *Frondina permica* Sellier de Civrieux & Dessauvagie. Section 3, 32: sample 121; 34: sample 113. Section 2, 33: sample 56. Section 1, 38: sample 26. 32-33, 38: X95; 34: X120.

Fig. 35-36, 39-40 - *Frondina* spp. Section 3, 35: sample 128. Section 1, 36: sample 9; 39: sample 51; 40: sample 11. 35-36: X110; 39: X95; 40: X115.

Fig. 37 - *Ichthyofrondina latilimbata* (Sellier de Civrieux & Dessauvagie). Section 1, sample 8, X115.

Fig. 41 - *Calvezina* sp. Section 1, sample 15, X100.

Fig. 42 - *Langella perforata* (Lange). Section 1, sample 15, X80.

Fig. 43 - *Frondinodosaria pyrula* Sellier de Civrieux & Dessauvagie. Section 3, sample 126, X95.

Fig. 45 - *Robuloides lens* Reichel. Section 1, sample 7, X150.

Fig. 46 - *Hemigordius* ? sp. Section 3, sample 132, X70.

Fig. 47 - *Hemigordius zaninettiae* Altiner. Section 1, sample 34, X75.

Fig. 48 - *Hemigordius* sp. Section 1, sample 32, X35.

Fig. 49 - *Multidiscus padangensis* (Lange). Section 2, sample 79, X95.

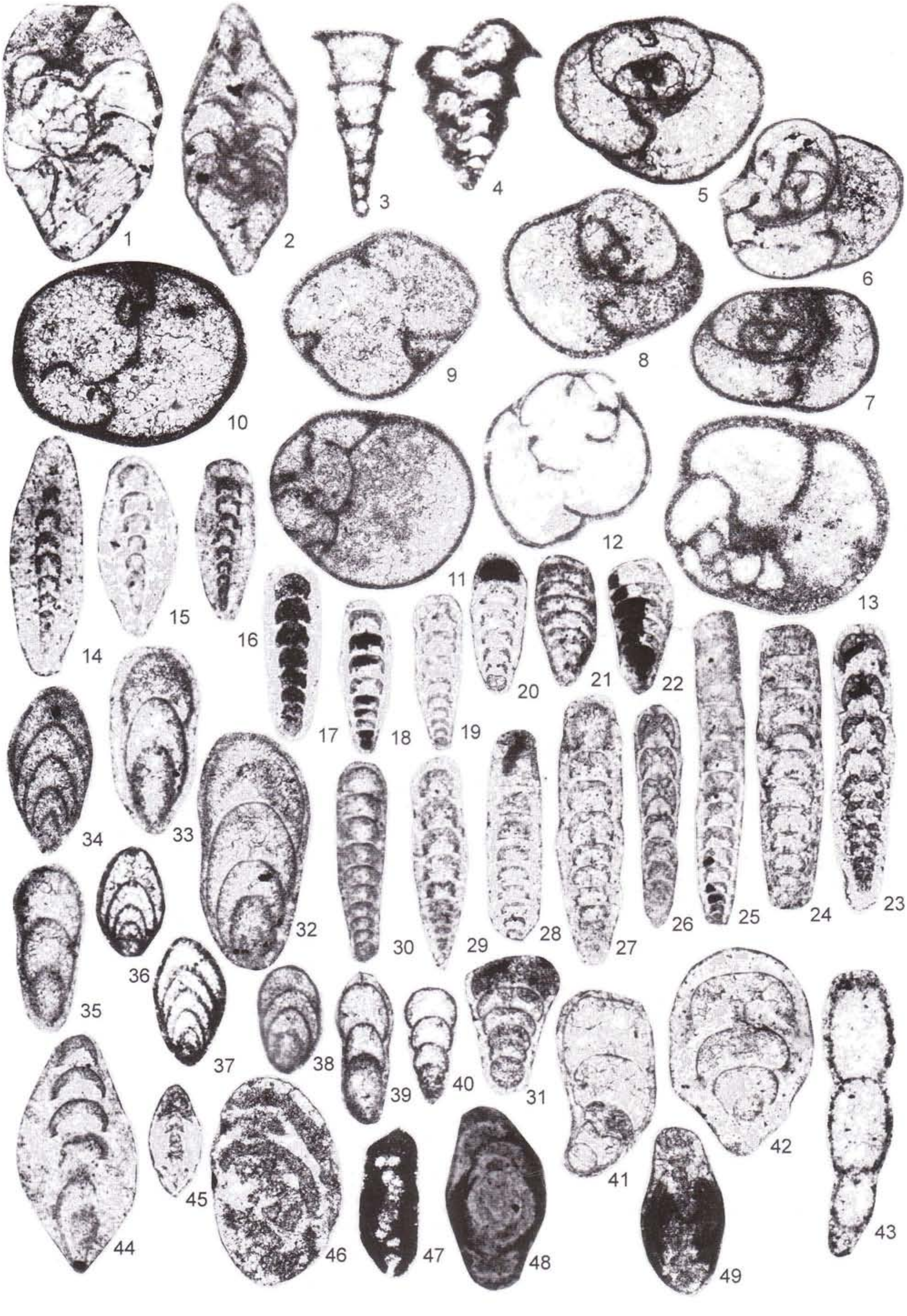
1
2
3
4
5
6
7
8
9
10
11
12
13
14
15
16
17
18
19
20
21
22
23
24
25
26
27
28
29
30
31
32
33
34
35
36
37
38
39
40
41
42
43
44
45
46
47
48
49

thonous material which are either oncolites (Pl. 2, figs. 16-18) or intraclasts (Pl. 2, fig. 15). These oncolites are quite similar to poorly sorted algal balls, algal pellet oncolites, coated bioclasts, cyanophyceae oncoides or algally coated-grains of various authors (Toomey & Cys 1977; Flügel 1982; Tisljar 1983; Catalov 1983). According to Tisljar (1983), such oncolites and associated intraclasts are brought in from adjacent shoals and redeposited onto the micritic layers. Algal fragments, micrite clasts and other small fragments of unknown origin are usually surrounded by blue-green algae which most probably created micrite envelops through boring activity. The black colour is considered to be formed also by the concentration of authigenic iron minerals. One possible mechanism for the formation of dark intraclasts was explained by Noe (1987) as the erosion of thalli of allochthonous algae filled with dark micrite.

Geinitzinid- and crinoid-rich argillaceous lime mudstone-wackestone lithofacies: this lithofacies is characterized by the abundance of broken crinoid stems and geinitzinid foraminifera (Pl. 3, fig. 1). The sediment was strongly affected by stylolitization and crinoid fragments resisted pressure solution. The calcareous algae is extremely rare in the facies.

Quartz-rich sandy limestone lithofacies: underlying the oolitic limestones of the uppermost Permian, this lithofacies consists of fine sand to silt sized quartz grains, many dark pellets, brachiopod fragments and few oncolites embedded in a sparry calcite cement (Pl. 3, figs. 2-3). Foraminifers are rare and calcareous algae are nearly absent in the facies. The quartz-rich sandy limestone lithofacies might have been deposited by storm-related currents or winds as suggested by Cirilli et al. (1998).

Oolitic grainstone lithofacies: this lithofacies characterizes the top of the Permian section. Recrystallized and well preserved ooids (Pl. 3, fig. 4-8) have been described from the latest Permian beds in a belt extending from Greenland through the western Paleotethys (Broglio Loriga et al. 1983; Neri & Pasini 1985; Noe 1987; Holser et al. 1991; Wignall & Hallam 1992, 1993; Andjelkovic et al. 1993; Cirilli et al. 1998; Heydari et al. 2001; Stemmerik 2001). The nuclei of these ooids are usually algal fragments or foraminifera shells. They are often dissolved and replaced by calcite crystals. In well washed oolitic facies (Pl. 3, fig. 7), the interparticle pores are filled with isopachous bladed calcite and drusy calcite cement, indicating freshwater diagenesis. In some levels of the oolitic section oolite-quartz grain aggregates are observed (Pl. 3, fig. 6). These aggregates resemble the grapestones of Scholle (1978) and coated pebbles of Paul & Peryt (2000) and are interpreted to have formed at times of increasing water movement conditions.

Stromatolitic boundstone lithofacies: resting with a sharp contact (Pl. 3, figs. 8-9) on the oolitic grainstone lithofacies, partially dissolved and recrystallized stromatolitic boundstones constitute the lowermost Griesbachian facies. Lithologically similar chronostratigraphic equivalents to this facies include Scythian stromatolites from various regions of Taurides in Turkey (Özgül 1976; Altiner et al. 1980, 2000; Altiner 1981, 1984; Zaninetti et al. 1981; Marcoux & Baud 1986; Köylüoğlu & Altiner 1989; Crasquin-Soleau et al. 2002), cryptalgal buildups of domal stromatolite type in Sovetashen (Armenia) (Baud et al. 1989), the *Lingula* stromatolites of the Uomo section and microspar with cryptalgal laminae in tidal flat facies in Tesero oolitic horizon in Italy (Noe 1987; Wignall & Hallam 1992), microbial mounds in Triassic rocks in Shah Raza and Abadeh sections in Iran (Heydari et al. 2001), Kalkowsky's stromatolites (Bundsandstein, Harz mountains) in Germany (Paul & Peryt 2000) and microbialite carbonate crust of South China (Kershaw et al. 1999). Basal Triassic stromatolitic laminae contain a large number of foraminiferal shells usually represented by two genera, *Rectocornuspira* and *Earlandia*.

PLATE 2

Fig. 1-3 - *Agathammina pusilla* (Geinitz). Section 1, 1, 3: sample 43. Section 2, 2: sample 75. 1-2: X80; 3: X50.

Fig. 4-8 - Staffellids. Section 2, 4: sample 79; 7: sample 76. Section 3, 5: sample 117; 6: sample 110. Section 1, 8: sample 22. 4-8: X40.

Fig. 9 - *Reichelina* sp. Section 3, sample 130, X150.

Fig. 10-12 - *Rectocornuspira kalhori* Brönnimann, Zaninettti & Bozorgnia. Section 2, sample 81, 10: X150; 11-12: X210.

Fig. 13 - *Earlandia* sp. Section 2, sample 83, X180.

Fig. 14 - Algal wackestone-packstone lithofacies. Note small broken fragments and large unbroken thalli of allochthonous algae whose central stems are filled with dark inhomogenous micrite, different than the groundmass. Section 1, sample 2, X24.

Fig. 15 - Mudstone-packstone lithofacies with oncolites and dark clasts. Section 1, sample 5, X24.

Fig. 16-18 - Oncolites in the mudstone-packstone lithofacies with oncolites and dark clasts. Section 1, 16: sample 16; 17-18: sample 35, X24.

Fig. 19 - Large coated gymnocodiaceans in the algal wackestone-packstone facies. Note the micritic matrix almost completely washed out. Section 1, sample 18, X24.

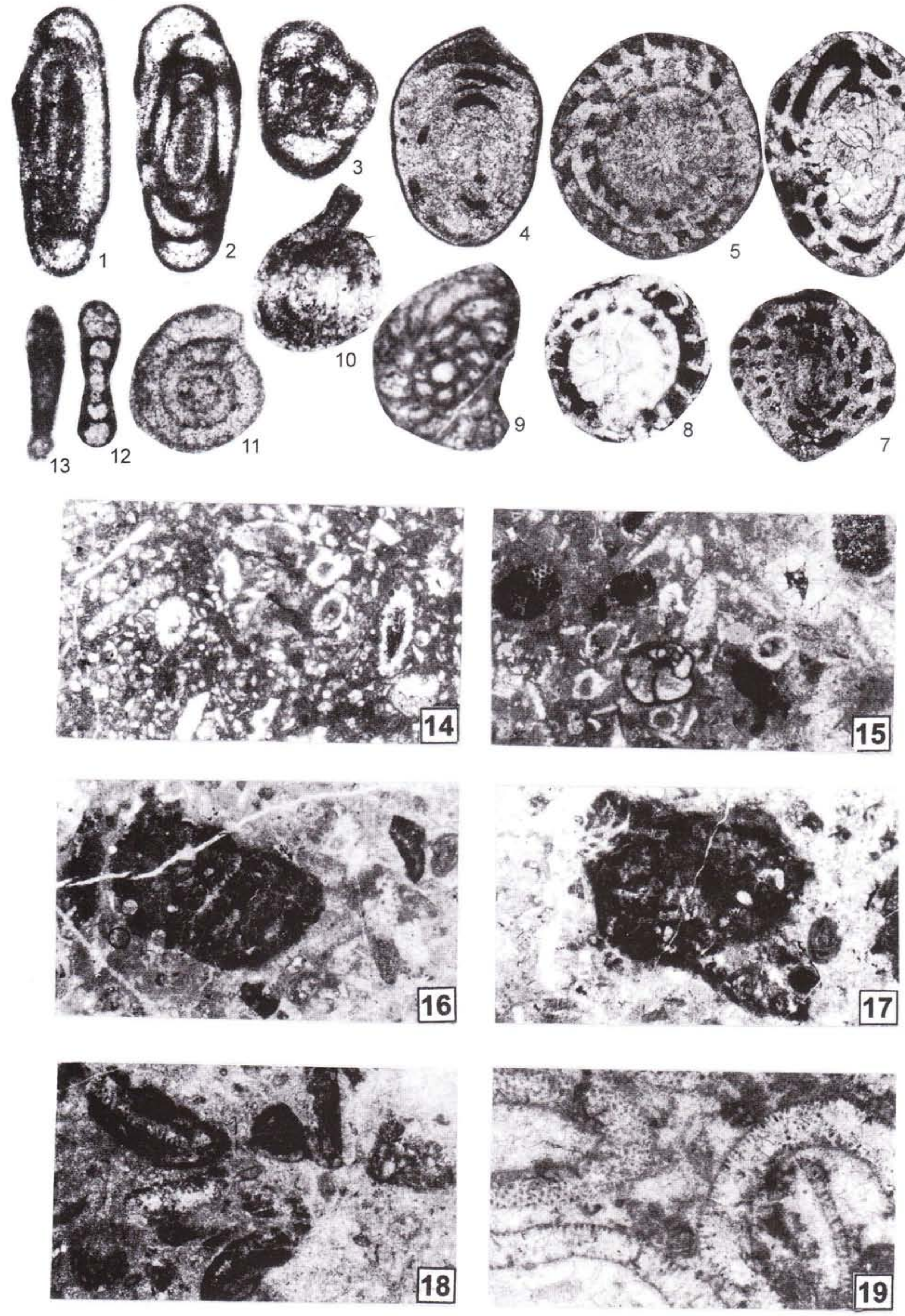

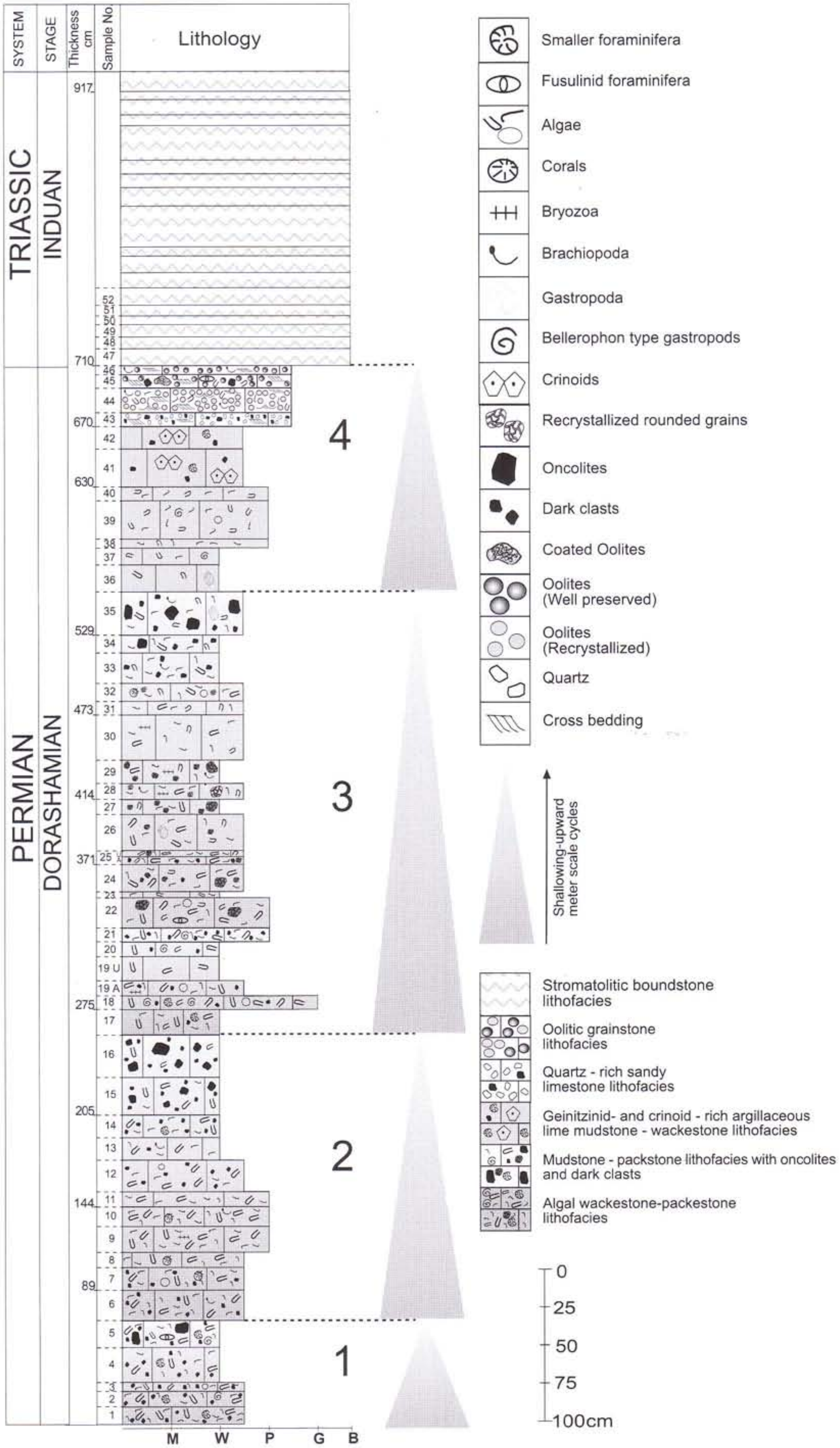

Fig. 4 - Principal measured section (section 1) showing the meter-scale cyclicity in uppermost Permian beds and overlying Triassic stromatolites.

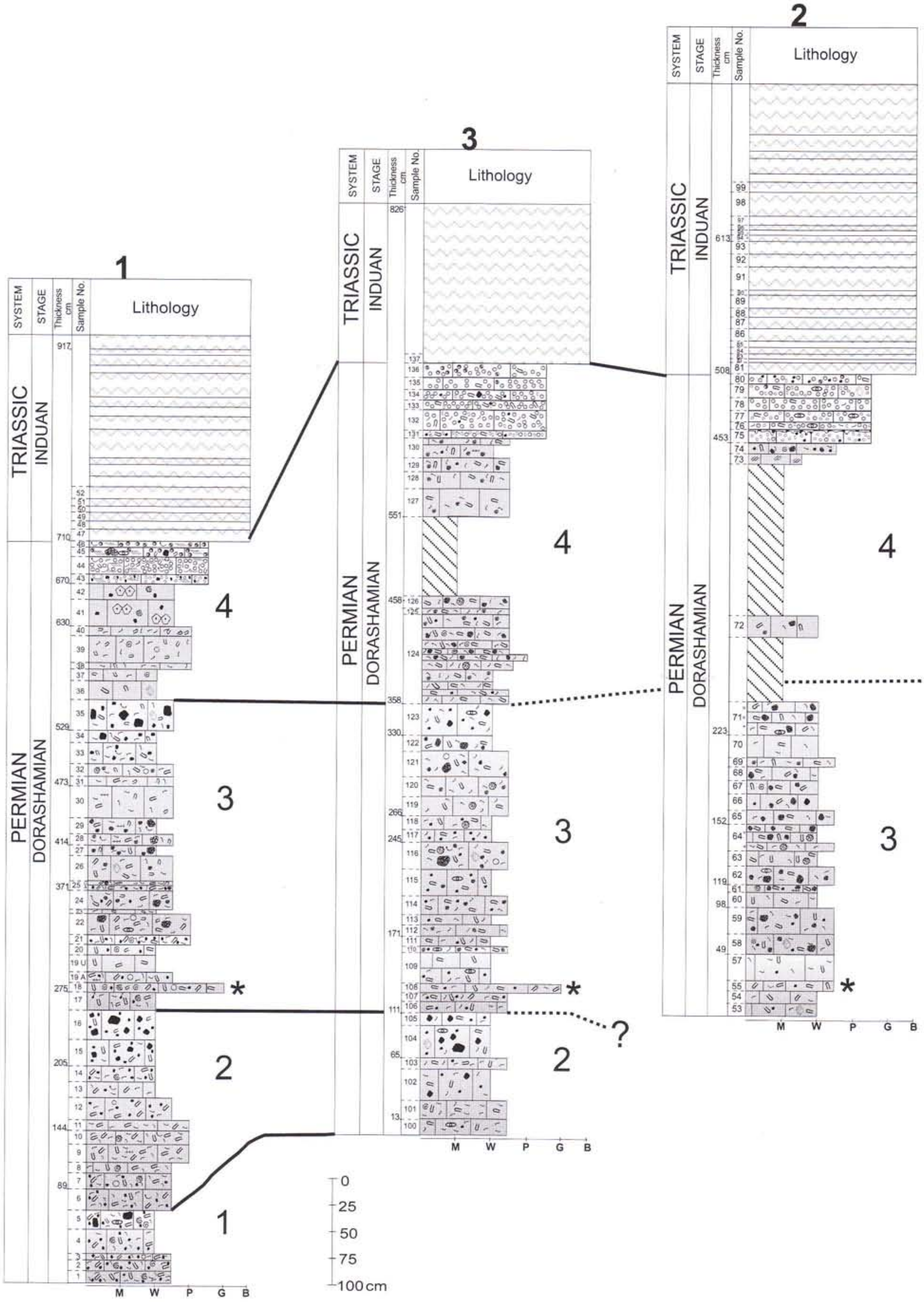

Fig. 5 - Correlation of parasequences (meter-scale cycles 1-4) recognized in three measured sections. Oblique hatches indicate covered intervals. The bed indicated with an asterisk is the marker level prominently observed in three sections and its microfacies is illustrated in Pl. 2, Fig. 19. For symbols and explanations, see Fig. 4.

Meter-scale cyclicity

The three sections measured through uppermost beds of the Permian in the Hadim region (central Taurides) consist mainly of subtidal carbonates capped by a distinct oolitic level (Figs. 4-5). Subtidal carbonates constitute basically meter-scale cycles measuring 2 or 3 m in thickness and are composed of an alternation of two main lithofacies reflecting distinct deepening and shallowing periods (parasequences 1-3). The deepening stage is usually characterized by the deposition of algal wackestone-packstone lithofacies well below the wave base. This facies grades upward into the mudstone-packstone lithofacies with oncolites and dark clasts deposited much closer to the wave base. Oncolites and dark clasts, possibly winnowed from zones above the wave base, are the strong evidence of shallowing in subtidal cycles. The absence of dissolution vugs, karst breccia, desiccation cracks and any carbonate deposit of tidal flat or beach type suggests that these cycles are incomplete and of subtidal type.

The last parasequence (4) overlying the subtidal parasequences (1-3, Figs. 4-5) commences also by the deposition of algal wackestone-packstone lithofacies indicating a sudden deepening in the succession. This facies grades upward into the geinitzinid- and crinoid-rich argillaceous lime mudstone-wackestone lithofacies by the progressive decrease in algal content. The upper half of the parasequence is characterized by the prograding quartz-rich sandy limestone lithofacies followed by recrystallized or well preserved oolitic grainstone beds deposited above the wave base. These oolitic levels are rippled and exhibit evidence of freshwater diagenesis. At the top of the parasequence ripple crests are truncated by erosion and overlain by stromatolites of Early Griesbachian age.

In order to test the response of organisms to cyclicity within studied successions we have carried out a number of counting experiments. The most evident response appeared in the 4th parasequence capped by oolitic grainstone lithofacies. Nearly all foraminiferal and algal groups declined in oolitic grainstones in comparison to their abundance in subtidal facies.

Among foraminifera, the response of *Paradagmarita* and geinitzinids is significant in subtidal parasequences (Fig. 6). For example, at the bases of parasequences 3 and 4, these foraminifers occur in their greatest abundance. The high frequency of foraminiferal occurrences coincides with an abrupt decline in oncolites and dark clasts, a pattern that is consistent with rapid deepening. However, this correlation is not evident for *Dagmarita* and *Globivalulina* whose abundances seem to be randomly distributed (Fig. 7).

Contrary to opinions of Nakazawa & Runnegar (1973) and Teichert (1990), we do not consider that faunal and floral biodevirsity declined gradually in the Middle and Late Permian. Foraminifers, for example, one of the most useful groups for detecting the Permian-Triassic boundary, flourished during the Midian (=Capitanian) transgression but, were partly eliminated at the Midian-Djulfian (=Wuchiapingian) boundary (Altiner 1984; Leven 1992). During the latest Permian (Djulfian and Dorashamian) most groups that escaped from the end-Midian extinction event stabilized (most biseriamminids, geinitzinids, hemigordiopsids and some fusuline groups, for example schubertellids) or even flourished by the addition of new taxa (*Paradagmarita*, various species of *Paleofusulina*). The apparent changes in diversity are related to regional facies variations and partly to provinciality. In our sections, for example, the rare occurrence of fusulines (except staffellids) has already been explained by the spectacular development of two marine biofacies belts bordering the Paleo-Tethys Ocean (Altiner et al. 2000). The Northern Biofacies Belt is characterized by a diversified fusuline assemblage even in the Djulfian and Dorashamian stages, whereas the Southern Biofacies Belt including the study area is characterized by the near absence of fusulinaceans. In this biofacies belt, meter-scale cycles are also responsible for faunal variations and, in case of sporadic sampling, this could lead to certain misinterpretations because of apparent increase or decrease of taxa due to the cyclicity. In our subtidal cycles close to the Permian-Triassic boundary the faunal decrease is not evident except variations in abundance of some special taxa. However, just below the Permian-Triassic boundary, since a marked facies restriction

PLATE 3

Fig. 1 - Geinitzinid- and crinoid-rich argillaceous lime mudstone-wackstone lithofacies. Note the absence of calcareous algae. Section 1, sample 42, X24.

Fig. 2-3 - Quartz-rich sandy limestone lithofacies. Note the abundance of dark pellets and brachiopod shells. The dark grain on the right side of the fig. 3 is an oncolite. Section 1, sample 43, X24.

Fig. 4-7 - Oolitic grainstone lithofacies. Various degrees of recrystallization and preservation indicate freshwater diagenesis in the facies. Large oolite-quartz grain aggregates are present in Fig. 6. Section 1, 4 - 5: sample 44; 6-7: sample 46. X24.

Fig. 8 - The P/T boundary (third-order sequence boundary). Stromatolitic boundstone lithofacies resting with a sharp contact on the oolitic grainstone lithofacies. Note truncated oolites. Section 3, sample 136, X24.

Fig. 9 - Partly dissolved and recrystallized stromatolitic boundstone lithofacies containing *Rectocornuspira kalhori*. Section 1, sample 47, X24.

Fig. 10 - The P/T boundary (third-order sequence boundary) illustrating the sharp contact between the oolitic grainstone and the overlying stromatolitic boundstone lithofacies. Coin for scale. Section 3.

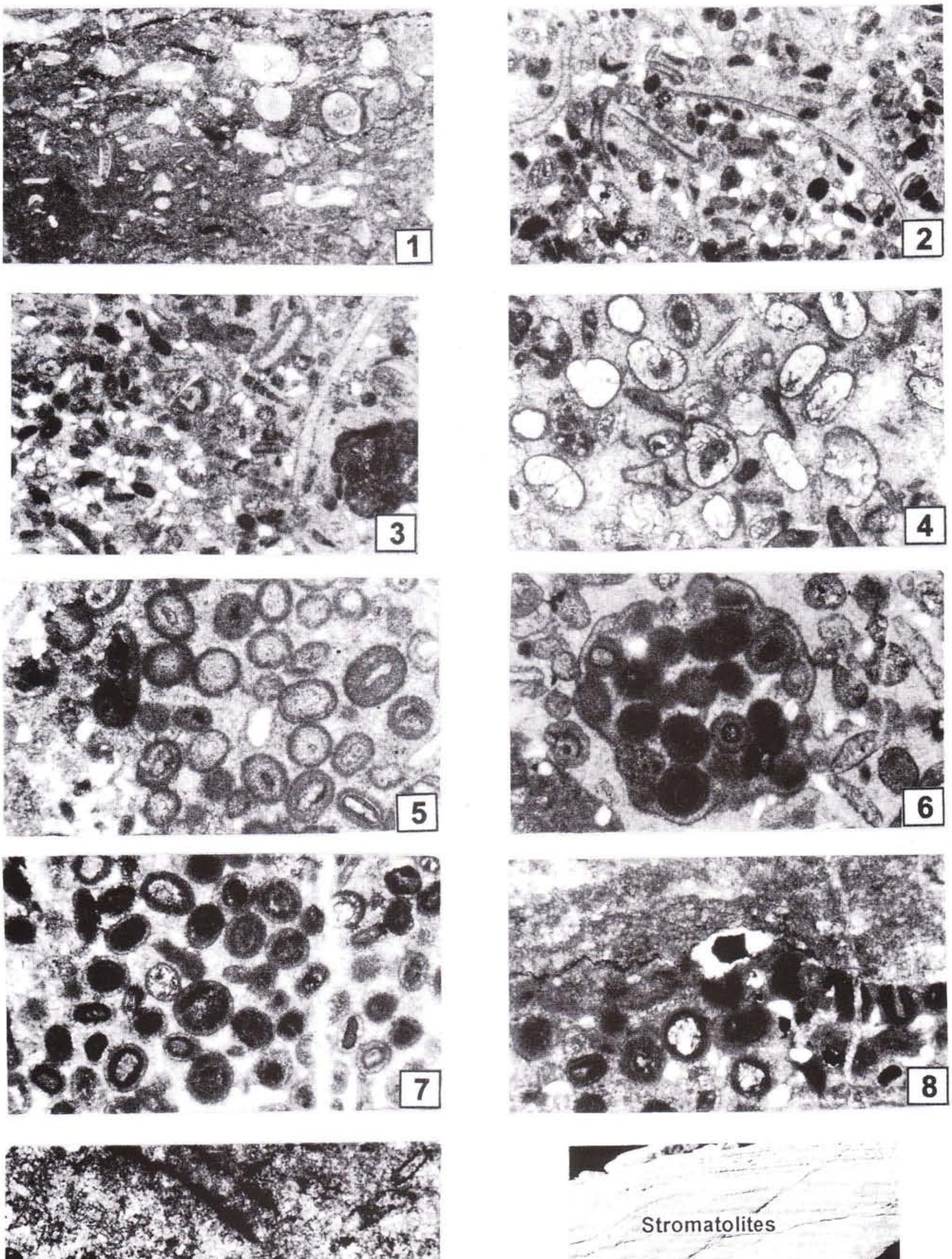
1
2
3
4
5
6
7
8
9
Stromatolites
Oolites
10

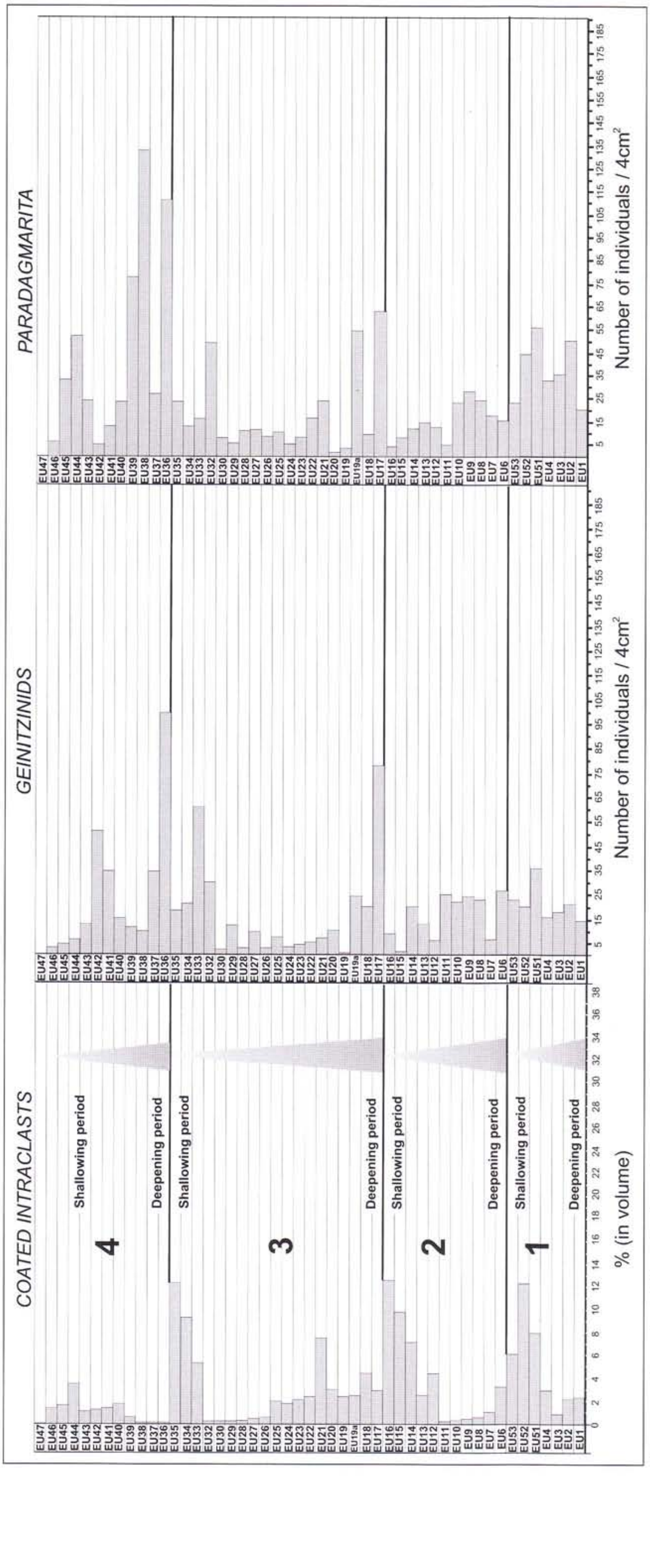

Fig. 6 - Comparison of the abundance of coated and dark intraclasts with the abundance of *Paradagmarita* and geinitzinid foraminifera in measured section 1. Note that the increase in the abundance of these taxa is generally inversely proportional with the increase of coated and dark intraclasts, which indicates parasequence tops.

occurred by the progradation of shoaling oolites, the biota was influenced from this change and markedly declined.

Sequence stratigraphic approach

The vertical stacking pattern of parasequences recognized in the three measured sections consists of three subtidal parasequences (1-3, Fig. 5), each characterized by a general upward increase in size of dark clasts and oncolites that were winnowed from zones above the wave base. The 4[th] parasequence (4, Fig. 5) consists of subaerially exposed oolites at the top of the Permian. These relations suggest that the Permian portion of sections represent highstand systems tract deposits within the sequence stratigraphic framework (Fig. 8). These highstand systems tract deposits, as well as uppermost Permian sections elsewhere in Turkey (Lys & Marcoux 1979; Altiner 1981, 1984, 1988; Altiner et al. 1980, 2000; Zaninetti et al. 1981; Marcoux & Baud 1986; Köylüoğlu & Altiner 1989; Crasquin-Soleau et al. 2002), were subaereally exposed due to an eustatic sea level fall close to the Permian-Triassic boundary, and a gap accounting for the absence of latest Dorashamian and earliest Griesbachian strata occurred. As interpreted in Fig. 8, this unconformity is a sequence boundary and corresponds in the Haq et al. (1987) chart to the top of the last Permian sequence. During maximum sea level fall corresponding to 252 m.y., the shallow subtidal carbonates of the Taurus Carbonate Platform must have been exposed, while shelf margin and then transgressive systems tract deposits of the overlying sequence were laid down to the north of the platform facing to the Paleo-Tethys Ocean

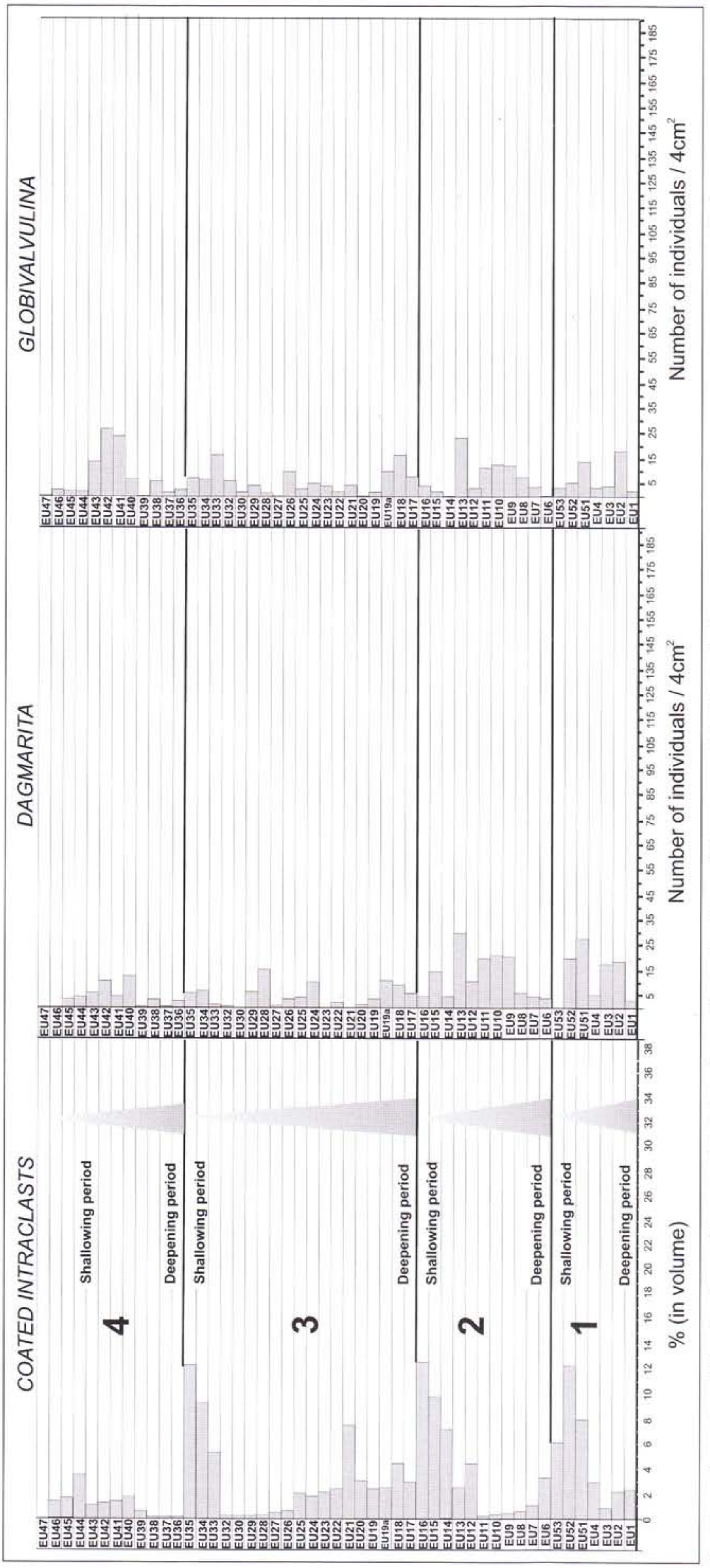

Fig. 7 - Comparison of the abundance of coated and dark intraclasts with the abundance of *Dagmarita* and *Globivalvulina* in measured section 1. Variation in the abundance of these taxa is not correlatable with the distribution of coated and dark intraclasts.

(Şengör & Yilmaz 1981; Şengör et al. 1988; Altiner et al. 2000). We interpret the Griesbachian stromatolites, directly overlying the Permian succession, as the shoreward facies of the transgressive systems tract deposits. The Permian-Triassic unconformity corresponds to an interval of erosion and nondeposition in the Permian, and to an interval of nondeposition at the base of the Triassic (Fig. 8). This also suggests that transgressive stromatolites might have been laid down diachronously, beginning in the latest Permian when the rate of eustatic rise increased.

Although the sequence stratigraphic interpretation presented in this study is perfectly logical, an alternate interpretation is possible for the Permian-Triassic boundary of central Taurides. This is the growing evidence for a catastrophic end to the Permian period (Wignall 2001; Becker et al. 2001; Kaiho et al. 2001; Lo et al. 2002; Reichow et al. 2002; Berner 2002; Zhou et al. 2002). According to this catastrophist model, independently of sea level fluctuations, some extrinsic event (bolide impact or massive eruption of flood basalt) caused the collapse of both terrestrial and marine ecosystems. In the shallow marine realm, normal carbonate factories were killed off and replaced by stromatolites. If Early Triassic stromatolites are "disaster forms" as maintained by Schubert & Bottjer (1992) then we would not expect to find Late Permian stromatolites anywhere in the Taurides, or Early Triassic normal marine carbonates laterally equivalent to the stromatolites.

The uppermost Yellice Member oolites of central Taurides and the oolites of the Tesero Horizon in Italy are found to be perfectly similar if the stratigraphic position and microfacies characteristics of these units are compared. Among several studies of the Permian-Triassic boundary in successions containing Yellice or Tesero type deposits in the Tethys (Altiner et al. 1980; Altiner 1981; Neri et al. 1986; Broglio-Loriga 1986a, b, 1988; Noe 1987; Wignall & Hallam 1992; Özgül 1997; Cirilli et al. 1998; Altiner & Özgül 2001; Crasquin-Soleau et al. 2002), that of Wignall & Hallam (1992) is the most significant from the sequence stratigraphy and cyclostratigraphy point of view.

These authors recognized a sequence boundary below the Tesero Oolite Horizon (Werfen Formation) and interpreted the uppermost Permian and the lowermost Griesbachian succession as transgressive deposits. In Fig. 9 we present a tentative correlation between the central Tauride and the north Italy sections because both localities are within the Southern Biofacies Belt of Altiner et al. (2000) and the prograding Permian oolites at the top of sections are nearly identical both in facies characteristics and age.

Our parasequence 4 seems to be equivalent to PAC (punctuated aggradational cycle) 1 of Wignall & Hallam (1992), which commences with the bioclastic limestone of the Bellerophon Formation and is capped by lower Tesero oolites.

The equivalent of PAC 2, still assigned to the Permian by Wignall & Hallam (1992), seems to be lacking in the Tauride section. If the unconformity between the Dorashamian (parasequence 4) and the stromatolites of Early Griesbachian age corresponds to the uppermost Permian type 2 sequence boundary in the Haq et al. (1987) chart, then the correlative conformity of the sequence boundary could correspond to the top of PAC 2 of Wignall & Hallam (1992). If so, the North Italian Permian section should have been laid down in relatively deeper water conditions in the Permian carbonate platform and the PAC 2 would mostly represent the aggradational shelf margin systems tract of the sequence. However, evidence contrary to this interpretation is the less restricted nature of the Permian fauna in the Tauride sections, suggesting a more offshore setting for our study area relative to the North Italian sections.

Discussion and conclusions

As we have demonstrated in this study, the Permian portion of the Permian-Triassic boundary beds in the central Tauride sections consists of meter-scale cycles. These cycles are mostly of subtidal type without any intervening intertidal and supratidal facies, indicating a certain shoaling or filling of the accomodation space.

These parasequences are typically aggradational, suggesting a more or less flat depositional surface in the carbonate platform. This wide carbonate platform is characterized by the monotonous Middle-Upper Permian deposits corresponding to the Southern Biofacies Belt of Altiner et al. (2000).

The rapid progradation of latest Permian oolites represents an abrupt shallowing of the depositional regime. A sequence boundary at the top of these oolites is an unconformity developed in the inner platform deposits. The correlative conformity may exist to the north of this platform, however, it cannot be easily recognized because of later tectonism which occurred during the Cretaceous and Tertiary (Özgül 1976; Şengör & Yilmaz 1981). When the position of the section is interpreted following the Haq et al. (1987) chart it is apparent that the Permian-Triassic boundary corresponds to a gap located between the Dorashamian oolites and the Griesbachian stromatolites.

Nearly all Permian foraminiferal and algal groups declined in oolitic grainstone lithofacies of central Taurides and became extinct below the stromatolites of Griesbachian age. The response of *Paradagmarita* and geinitzinids have been found remarkable in the subtidal cycles. These foraminifers tend to occur in their greatest abundance at the base of parasequences corresponding to the rapid deepening trend during times of sea level rise.

Finally, parasequences that we distinguished in the central Tauride sections are correlatable with PACs of Wignall & Hallam (1992) described in the northern Italian (Tesero) sections. If this correlation is correct, however, the sequence boundary defined by these authors could be considered higher than the level defined at the base of their PAC 1 corresponding to the uppermost levels of the Bellerophon Formation.

Acknowledgements. This study is part of a scientific research on Upper Paleozoic Stratigraphy and Micropaleontology of Turkey supported by the Scientific and Technical Reseach Council of Turkey (Project No: TUBITAK-YDABAG 100Y040). We are grateful to Dr. John R. Groves (University of Northern Iowa, USA) who read and critically reviewed the manuscript.

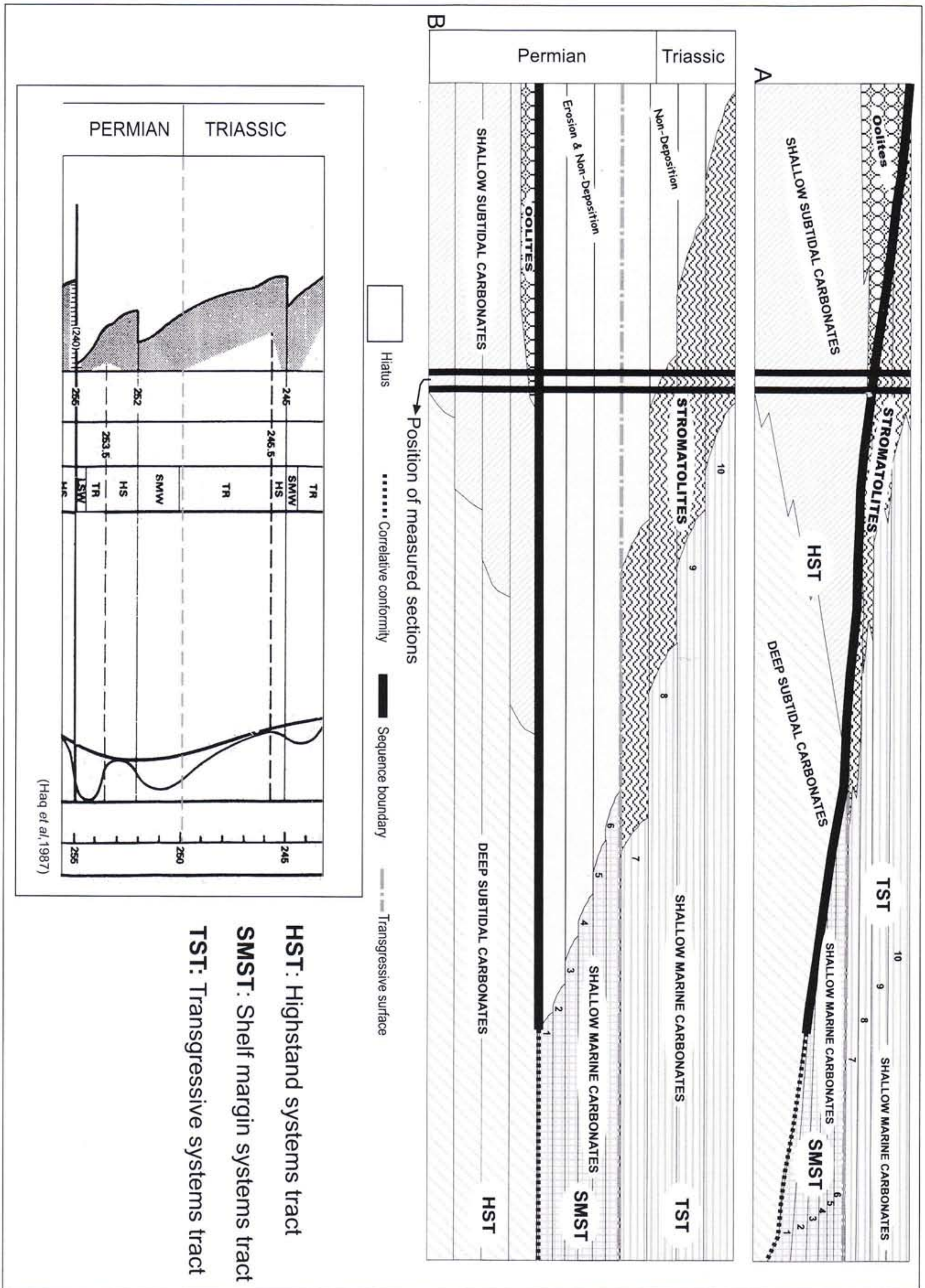

Fig. 8 - Sequence stratigraphic scenario showing the hypothetical cross section (A) and the chronostratigraphic interpretation (B) in the study area. Sea level curve at the Permian-Triassic boundary is from Haq et al. (1987)

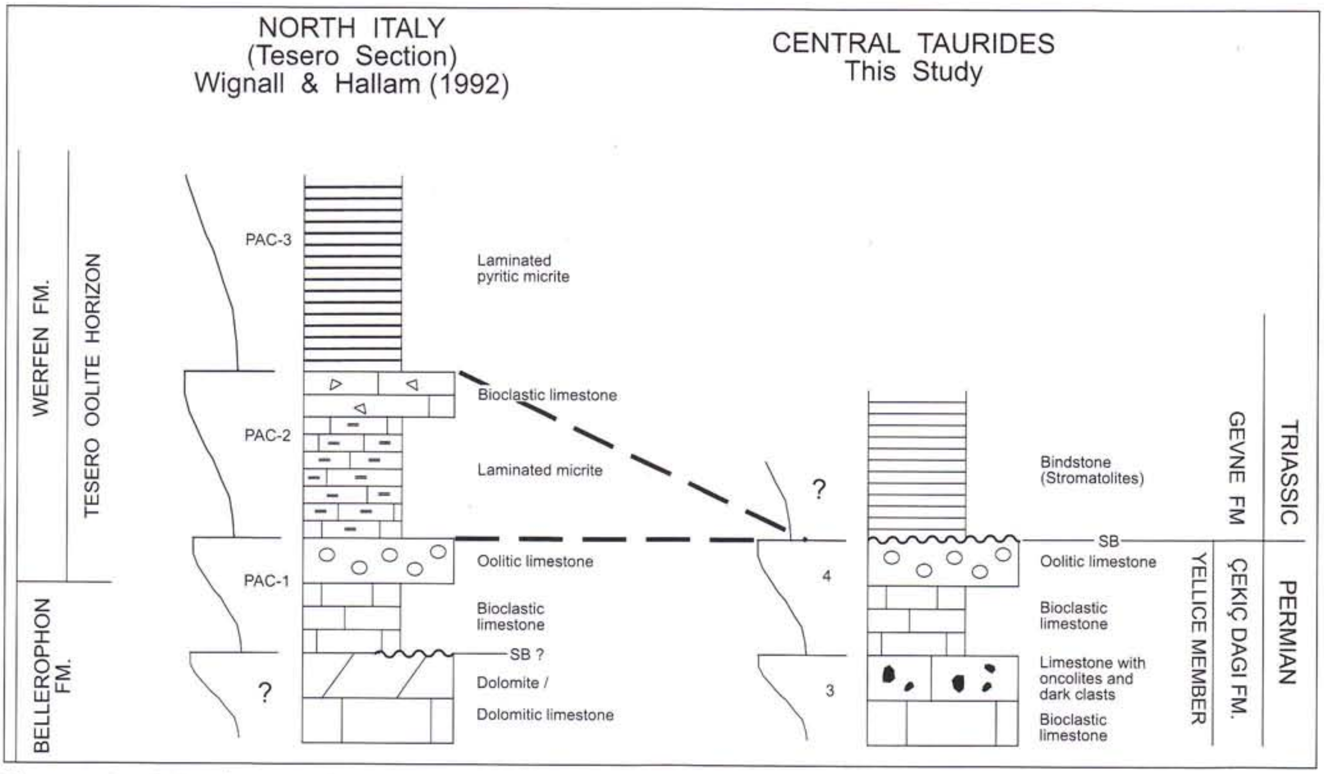

Fig. 9 - Correlation of punctuated aggradational cycles (PACs) recognized in North Italy sections (Wignall & Hallam, 1992) with parasequences of Central Taurides. Note that the sequence boundary recognized in this study is correlatable with the top of the PAC-2.

REFERENCES

Altiner D. (1981) - Recherches stratigraphiques et micropaléontologiques dans le Taurus Oriental au NW de Pinarbaşı (Turquie). Thesis (unpublished), Univ. Genève, Thèse No. 2005: 450pp., Genève.

Altiner D. (1984) - Upper Permian foraminiferal biostratigraphy in some localities of the Taurus Belt. In Tekeli O. & Göncüoğlu M.C. (Eds.) - Geology of the Taurus Belt. *Proc. Int. Tauride Symp.*, 255-268, Ankara.

Altiner D. (1988) - Pseudovidalinidae n. fam. and *Angelina* n. gen. from the Upper Permian of south and southeast Turkey: *Rév. Paléobiologie, Sp. Vol.* 2 (Benthos '86): 25-36, Genève.

Altiner D., Baud A., Guex J. & Stampfli G. (1980) - La limite Permien-Trias dans quelques localités du Moyen-orient: recherches stratigraphiques et micropaléontologiques. *Riv. It. Paleont. Strat.*, 101: 235-248, Milano.

Altiner D. & Özgül N. (2001) - Carboniferous and Permian of the allochthonous terranes of the Central Tauride Belt. International Conference on Paleozoic Benthic Foraminifera, Guide Book: 35 p., Ankara.

Altiner D., Özkan-Altıner S. & Koçyiğit A. (2000) - Late Permian foraminiferal biofacies belts in Turkey: paleogeographic and tectonic implications. In: Bozkurt E., Winchester J. A. & Piper J. D. A. (eds), Tectonics and Magmatism in Turkey and the Surrounding Area. *Geol. Soc. London, Sp. Publ.*, 173: 83-96, London.

Andjelkovic M., Pesic L. & Andjelkovic D. (1993) - The Permian/Triassic boundary in the Dinarides. *Ann. Geol. Penins. Balk.*, 57, 1: 1-20, Beograd.

Baud A., Magaritz M. & Holser W. T. (1989) - Permian-Triassic of the Tethys: Carbon Isotope studies. *Geol. Rund.*, 78(2): 649-677, Stuttgart.

Becker L., Poreda R. J., Hunt A. G., Bunch T. E. & Rampino M. (2001) - Impact event at the Permian-Triassic boundary: evidence from extraterrestrial noble gases in fullerenes. *Science*, 291: 1530-1533, Washington.

Berner R. A. (2002) - Examination of hypotheses for the Permo-Triassic boundary extinction by carbon cycle modelling. *Proc. Nat. Ac. Sciences USA*, 99 (7): 4172-4177, Washington.

Beukes N. J. (1983) - Ooids and oolites of the proterophytic Boomplaas Formation, Transvaal Supergroup, Griqualand West, South Africa. In Peryt T. (Ed.) - Coated Grains, 566-575, (Springer) Berlin-Heidelberg-New York.

Blumental M. M. (1947) - Geologie der Tauruskettenim Hinterland von Seydişehir un Beyşehir. *Maden Tetkik Arama Dergisi*, Seri D, 2: 242 pp., Ankara.

Blumental M. M. (1951) - Batı Toroslar'da Alanya ard ülkesinde jeolojik araştirmalar. *Maden Tetkik ve Arama Enst.*, Seri D, 5: 1-134, Ankara.

Broglio Loriga C., Conti M. A., Farabegoli E., Fontana D., Mariotti N., Massari F., Neri C., Nicosia U., Pasini M., Perri M. C., Pittau P., Posenato R., Venturini C. & Viel G. (1986a) – Upper Permian and P/T boundary in the area between Carnia and the Adige Valley. In: Permian and Permian-Triassic Boundary in the South-Alpine Segment of the Western Tethys. IGCP Project 203. *Excursion Guidebook*, 23-28, Brescia.

Broglio Loriga C., Fontana D., Massari F., Neri C., Pasini M. & Posenato R. (1986b) – The Upper Permian sequence and the P/T boundary in the Sass de Putia Mt. (Dolomites). In: Permian and Permian- Triassic Boundary in the South Alpine Segment of the Western Tethys. IGCP Project 203. *Excursion Guidebook*, 73-90, Brescia.

Broglio Loriga C., Masetti D. & Neri C. (1983) - La Formazione di Werfen (Scitico) della Dolomiti occidentali: Sedimentologia e biostratigrafia. *Riv. Ital. Paleont. Strat.*, 88(4): 501-598, Milano.

Broglio Loriga C., Neri C., Pasini M. & Posenato R. (1988) – Marine fossil assemblages from Upper Permian to Lowermost Triassic in the Western Dolomites (Italy). *Mem. Soc. Geol. Ital.*, 34: 5-44, Roma.

Broglio Loriga C., Neri C. & Posenato R. (1986c) – The early macrofaunas of the Werfen Formation and the Permian-Triassic boundary in the Dolomites (Southern Alps, Italy) *Stud. Trent. Sci. Nat., Acta Geol.*, 62: 3-18, Trento.

Catalov G. A. (1983) – Triassic oncoids from Central Balkanides (Bulgaria). In Peryt T. (Ed.) – Coated Grains, 398-408, (Springer) Berlin-Heidelberg-New York.

Cirilli S., Radrizzani C. P., Ponton M. & Radrizzani S. (1998) – Stratigraphical and palaeoenvironmental analysis of the Permian-Triassic transition in the Badia Valley (Southern Alps, Italy). *Palaeogeogr.,Palaeoclimatol., Palaeoecol.*, 138: 85-113, Amsterdam.

Crasquin-Soleau S., Richoz S., Marcoux J., Angiolini L., Nicora A. & Baud A. (2002) – Les événements de la limite Permien-Trias: derniers survivants et/ou premiers re-colonisateurs parmi les ostracodes du Taurus (Sud-Ouest de la Turquie). *C. R. Geoscience,* 334: 489-495, Paris.

Flügel E. (1982) – Microfacies analysis of limestones. 633 pp., 53 pls., 78 figs., 58 tab., (Springer) Berlin-Heidelberg-New York.

Haq B. U., Hardenbol J. & Vail P. R. (1987) – Chronology of fluctuating sea level since Triassic. *Science*, 235: 1156-1160, Washington.

Heydari E., Wade W. J. & Hassanzadeh J. (2001) – Diagenetic origin of carbon and oxygen isotope compositions of Permian-Triassic boundary strata. *Sedimentary Geology*, 143: 191-197, Amsterdam.

Holser W. T., Schonlaub H. P., Boeckelmann K., Magaritz M. & Orth C. J. (1991) – The Permian- Triassic of the Gartnerkofel-1 core (Carnic Alps, Austria): Synthesis and conclusions. *Abh. Geol. Bundesanst.*, 45: 213-232, Wien.

Hongfu Y., Kexin Z., Jinnan T., Zunyi Y. & Shunbao W. (2001) – The global stratotype section and point (GSSP) of the Permian-Triassic boundary. *Episodes*, 24(2): 102-114, Beijing.

Jin Y., Wardlaw B. R. & Glenister B. F. (1997) – Permian chronostratigraphic subdivisions. *Episodes,* 20: 10-15, Beijing.

Kaiho K., Kajiwara Y., Nakano T., Miura Y., Kawahata H., Tazaki K., Ueshima M., Chen Z. Q. & Shi G. R. (2001) - End-Permian catastrophe by a bolide impact: evidence of a gigantic release of sulfur from the mantle. *Geology*, 29 (9): 815-818, Boulder.

Kershaw S., Zhang T. & Lan G. (1999) - A ?microbialite carbonate crust at the Permian-Triassic boundary in South China, and its palaeoenvironmental significance. *Palaeogeogr., Palaeoclimatol., Palaeoecol.*, 146: 1-18, Amsterdam.

Köylüoğlu M. & Altiner D. (1989) – Micropaléontologie (Foraminifères) et biostratigraphie du Permien supérieur de la région d'Hakkari (SE Turquie). *Rev. Paléobiologie*, 8: 467-503, Genève.

Leven E. Ja. (1992) – Problems of Tethyan Permian stratigraphy: *Intern. Geology Review*, 34 (10): 976-985, Columbia.

Lo C. H., Chung S. L., Lee T. Y. & Wu G. Y. (2002) – Age of the Emeishan flood magmatism and relations to Permian-Triassic boundary events. *EPSL*, 198 (3-4): 449-458, Amsterdam.

Lys M. & Marcoux J. (1978) – Le niveaux du Permien superiéur des Nappes d'Antalya (Taurides occidentales, Turquie). *C. R. Ac. Sciences*, Ser. D, 286: 1417-1420, Paris.

Marcoux J. & Baud A. (1986) – The Permo-Triassic boundary in the Antalya Nappes (western Taurides, Turkey). *Mem. Soc. Geol. It.*, 34: 243-252, Roma

Nakazawa K. & Runnegar B. (1973) – The Permian-Triassic boundary: a crisis for bivalves? In: A. Logan and L. V. Hills (Eds) – The Permian and Triassic systems and their mutual boundary. *Mem. Can. Soc. Petr. Geol.*, 2: 608-621, Ottawa.

Neri C. & Pasini M. (1985) – A mixed fauna at the Permian-Triassic boundary, Tesero Section, western Dolomites (Italy). *Boll. Soc. Paleont. Ital.*, 23 (1): 113-117, Modena.

Neri C., Pasini M. & Posenato R. (1986) – The Permian-Triassic boundary and the early Scythian sequence – Tesero section, Dolomites. In: Permian and Permian-Triassic boundary in the south-Alpine segment of the Western Tethys. IGCP 203, *Excursion Guidebook*, 111-116, Brescia.

Noe S. U. (1987) – Facies and paleogeography of the marine Upper Permian and of the Permian-Triassic boundary in the southern Alps (Bellerophon Formation, Tesero Horizon). *Facies,* 16: 89-142, Erlangen.

Özgül N. (1971) – Orta Torosların kuzey kesiminin yapisal gelişiminde blok hareketlerinin önemi. *Türkiye Jeol. Kur. Bült.*, 14: 75-87, Ankara.

Özgül N. (1976) – Some geological aspects of the Taurus orogenic belt-Turkey: *Bull. Geol. Soc. Turkey,* 19: 65-78, Ankara.

Özgül N. (1984) – Stratigraphy and tectonic evolution of the central Taurides. *Symposium on the Geology of the Taurus Belt,* 77-90, Ankara.

Özgül N. (1997) – Stratigraphy of the tectono- stratigraphic units in the region Bozkır-Hadim-Taşkent (northern central Taurides). *Maden Tetkik Arama Dergisi*, 119: 113-174 (in Turkish with English abstract), Ankara.

Paul J. & Peryt T. M. (2000) – Kalkowsky's stromatolites revisited (Lower Triassic Buntsandstein, Harz Mountains, Germany). *Palaeogeogr., Palaeoclimatol., Palaeoecol.,* 161: 435-458, Amsterdam.

Reichow M. K., Saunders A. D., White R. V., Pringle M. S., Al'Mukhamedov A. I., Medvedev A. I. & Kirda N. P. (2002) – Ar-40/Ar-39 dates from the West Siberian Basin: Siberian flood basalt province doubled. *Science*, 296: 1846-1849, Washington.

Scholle P. A. (1978) - A color illustrated guide to carbonate rock constituents, textures, cements and porosities. *AAPG Memoir* 27: 241 pp., Oklahoma.

Schubert J. K. & Bottjer D. J. (1992) - Early Triassic stromatolites as post mass extinction disaster forms. *Geology*, 20 (10): 883-886, Boulder.

Stemmerik L. (2001) - Sequence stratigraphy of a low productivity carbonate platform succession: the Upper Permian Wegener Halvo Formation, Karstryggen Area, East Greenland. *Sedimentology*, 48: 79-97, Oxford.

Şengör A. M. C. & Yilmaz Y. (1981) - Tethyan evolution of Turkey: a plate tectonic approach. *Tectonophysics*, 75: 181-241, Amsterdam.

Şengör A. M. C., Altiner D., Cin A., Ustaömer T.& Hsü K. J. (1988) - Origin and assembly of the Tethyside orogenic collage at the expense of Gondwana Land. In: Audley-Charles M. G. & Hallam A. (eds) - Gondwana and Tethys. *Geological Soc. London, Sp. Publ.*, 37: 119-181, London.

Teichert C. (1990) - The Permian-Triassic boundary revisited. In: E. G. Kauffman and O. H. Walliser (Eds), Extinction Events in Earth History. *Lect. Notes Earth Sci.*, 30: 199-238.

Tisljar J. (1983) - Coated grains facies in the Lower Cretaceous of the Outer Dinarides (Yugoslavia). In Peryt T. (Ed.) - Coated Grains, 566-575, (Springer) Berlin-Heidelberg-New York.

Toomey D. F. & Cys J. M. (1977) - Spirorbid/algal stromatolites, a probable marginal marine occurrence from the Lower Permian of the New Mexico, USA. *N. Jb. Geol. Palaont. Mh.*, 6: 331-342, Stuttgart.

Wignall P. B. (2001) - Large igneous provinces and mass extinctions. *Earth-Science Reviews*, 53 (1-2): 1-33, Amsterdam.

Wignall P. B. & Hallam A. (1992) - Anoxia as a cause of the Permian/Triassic mass extinction: facies evidence from northern Italy and the western United States. *Palaeogeogr., Palaeoclimatol., Palaeoecol.*, 93: 21-46, Amsterdam.

Wignall P. B. & Hallam A. (1993) - Griesbachian (earliest Triassic) palaeoenvironmental changes in the Salt Range, Pakistan and southeast China and their bearing on the Permo-Triassic mass extinction. *Palaeogeogr., Palaeoclimatol., Palaeoecol.*, 102: 215-237, Amsterdam.

Zaninetti L. & Altiner D. (1981) - Les Biseriamminidae (foraminifères) dans le Permien supérieur mésogéen: évolution et biostratigraphie. *Notes Lab. Paléont. Univ. Genève*, 2 (5): 27-31, Genève.

Zaninetti L., Altiner D. & Çatal E. (1981) - Foraminifères et stratigraphie dans le Permien supérieur du Taurus oriental, Turquie. *Notes Lab. Paléont. Univ. Genève*, 7(1): 1-37, Genève.

Zhou M. F., Malpas J., Song X. Y., Robinson P. T., Sun M., Kennedy A. K., Lesher C. M. & Keays R. P. (2002) - A temporal link between the Emeshian large igneous province (SW China) and the end-Guadalupian mass extinction. *EPSL*, 196 (3-4): 113-122, Amsterdam.